PARAMETERIZATION OF CUMULUS AND MCSs IN GCMs TO MESOSCALE MODELS

William R Cotton, Hongli Jiang, Scot C R Rafkin[1], G David Alexander[2], Ray L McAnelly
Colorado State University
Dept. of Atmospheric Science
Fort Collins, Colorado, USA

Summary: A scheme for parameterizing the influence of deep convective clouds and the organized mesoscale flow branches of mesoscale convective systems (MCSs) in mesoscale to global numerical weather prediction models is described. The deep convective component of the scheme is a hybrid mass flux and adjustment scheme. The mass flux component of the scheme resembles the Arakawa-Schubert scheme in which cloud warming and drying are a result of cumulus-induced subsidence and detrainment. The adjustment term has the effect of nudging the grid-averaged properties toward or away from cloud properties depending on whether the sub-cloud-ensemble is expanding or contracting. A probability density function is introduced to define the fraction of the cloud ensemble that is actually active within a grid box of limited area. The scheme is calibrated and tested with data obtained in cloud-resolving simulations of ordinary cumuli and cumulonimbi.

The MCS component of the scheme provides the heating, moistening, and momentum transports associated with the more slantwise, ascending and descending flow branches of the MCS. Cloud-resolving simulations of MCSs are used to obtain vertical profiles of heating and moistening rates associated with these slantwise flow branches. The scheme is tested with independent data from the cloud-resolving simulations. The decision to activate and de-activate the MCS scheme is based on the magnitude of predicted, vertically-integrated mesoscale kinetic energy which is related to conversion from deep convective clouds and internal energy sources and sinks associated with the developing flow branches.

1. INTRODUCTION

Our goal in this study is to develop a parameterization scheme of cumulus clouds and mesoscale convective systems (MCSs) that can be used in models having a wide range of grid spacings. In RAMS (*Pielke et al.*, 1993) we use interactive grid nesting in which a given model simulation may have grid spacings from 80 km down to cloud-resolving scales of a few kilometers or less. For example, using nest ratios of 4-to-1, grids may have spacings of 80 km, 20 km, 5 km, and 1.25 km, respectively. We seek a cumulus parameterization scheme that can be realistically applied to grids #1-3 without any user-defined changes in parameters or algorithms. Moreover, we also seek a parameterization scheme that treats not only deep upright convection but also heating, moistening, and momentum transports associated with the more slantwise motions in MCSs. This latter component of the scheme would be used in general circulation models (GCMs) that do not have sufficient resolution to depict those circulations explicitly. A desirable feature of the MCS component of the scheme is that it be interactive with the deep upright convective parameterization scheme and that it be turned on and

[1]Current Affiliation: University Corporation for Atmospheric Research, COMET, Boulder, CO 80307
[2]Current Affiliation: NASA/Goddard Space Flight Center, Code 978, Greenbelt, MD 20771

off based on predictions by the deep convection scheme and by the internal physics associated with MCSs.

Our first-generation deep convection parameterization scheme was developed by *Weissbluth and Cotton* (1993). It was designed specifically for use in mesoscale models with grid spacings less than 50 km. The scheme uses grid-point predicted vertical velocity variance that is based on a generalization of TKE-type closure models to deep convection for closure of several aspects of the parameterization. A single "characteristic" cloud model is also used to determine heating/moistening rates through a grid column and source functions of hydrometeor species for the host model. The cloud model was constructed from guidance obtained from cloud-resolving simulations of steady, intense cumulonimbi.

There are several deficiencies of this scheme which motivated us to develop a more general scheme. First it is not suitable for use in models having grid spacings coarser than 50 km. Second, since it is based on a single "characteristic" cloud that was calibrated for intense, steady cumulonimbi, it does not treat the more transient, towering cumuli and ordinary cumulonimbi properly when tested against cloud-resolving simulations of Florida sea breeze convection. Third, the scheme is computationally expensive since the grid-point predicted vertical velocity variance is constrained by its diffusion-limited linear stability criteria thus relatively small time steps are required for fine vertical grid spacings.

It was therefore decided to construct a new scheme that includes an ensemble of cumuli and only predicts the two-dimensional, vertically-integrated cumulus kinetic energy.

2. THE CUMULUS PARAMETERIZATION SCHEME

The cumulus parameterization scheme developed by *Rafkin* (1996) is a hybrid mass flux and adjustment scheme. The mass flux component of the scheme closely follows the *Arakawa and Schubert* (1974; hereafter *AS74*) parameterization to describe the cumulus-induced subsidence and detrainment.

Our experience with the Weissbluth scheme and the Kuo scheme suggests that the use of only one type of cloud, usually the deepest possible cloud, can lead to poor representations of cloud heating and moistening rates, particularly where cumulus clouds ranging from towering cumuli to ordinary cumulonimbi are predominant. Therefore, we introduce a new philosophical approach which makes use of a cloud probability density function. First we define the "cloud ensemble" to be the set of all possible cloud types which could exist in a given environment. We also define the "active cloud population" to be the subset of the cloud ensemble which actually exists in a given area or grid box. In some cases, such as in coarse-resolution GCMs, the active population will be the cloud ensemble.

This is what Arakawa and Schubert assumed. As the area under consideration shrinks, however, it will become physically impossible to contain all possible clouds in the sample area or grid square. We therefore introduce a probability density function to define what the active population of clouds can be within a grid box of limited area.

The first task in developing the new parameterization was to develop a set of equations which describes the effect of clouds and the environment on the model-resolved variables, and to use these equations as the basis for the parameterization. We begin with the assumption that there exists a function (G) which takes as arguments the cloud and environment properties and fractional areas and returns the model resolved property. We have chosen a simple, linear form of G:

$$G(\sigma_u^i, \sigma_d^i, \chi_u^i, \chi_d^i, \tilde{\chi}) = \overline{\chi} = \sum_{clouds} \sigma_u^i \chi_u^i + \sum_{clouds} \sigma_d^i \chi_d^i + (1 - \sigma_c)\tilde{\chi} \tag{1}$$

where $\overline{\chi}$ is the model resolved property, $\sigma_{u,d}^i$ is the updraft or downdraft cloud fractional area of cloud i, $\tilde{\chi}$ is the environment property, σ_c is the total cloud fractional area, and subscripts u and d refer to cloud updrafts and downdrafts, respectively.

Since we are interested in the time evolution of $\overline{\chi}$, we take the local time derivative, rearrange some terms and obtain

$$\frac{\partial \overline{\chi}}{\partial t} = \sum_{clouds} \left[(\chi_u^i - \tilde{\chi}) \frac{\partial \sigma_u^i}{\partial t} \right] + \sum_{clouds} \left[(\chi_d^i - \tilde{\chi}) \frac{\partial \sigma_d^i}{\partial t} \right]$$
$$+ (1 - \sigma_c) \frac{\partial \tilde{\chi}}{\partial t} + \sum_{clouds} \left(\sigma_u^i \frac{\partial \chi_u^i}{\partial t} \right) + \sum_{clouds} \left(\sigma_d^i \frac{\partial x_d^i}{\partial t} \right) \tag{2}$$

We posit that Eq. (2) should be used to parameterize the effect of cumulus convection upon the model-predicted variables. The first two terms on the r.h.s. of Eq. (2) may be regarded as adjustment terms, the third term as a subsidence term and remaining two terms as transient cloud terms. For simplicity, the transient cloud terms are neglected in this parameterization closure.

As in *Randall and Pan* (1993) we relax the equilibrium closure assumption used in *AS74* to determine the cloud-base ($z = z_o$) mass flux which is defined as

$$M_B = \rho(z_o) w(z_o) \sigma_*(z_o). \tag{3}$$

The sub-ensemble fractional area (σ_*) is defined over an area which is large enough to contain the ensemble of clouds, but small enough so as to cover only a fraction of a large-scale disturbance. The closure begins with the cumulus kinetic energy budget equation for a sub-ensemble as discussed by

Lord and Arakawa (1980) re-written in slightly different notation:

$$\frac{\partial}{\partial t}CKE(\lambda) = M_B(\lambda)A(\lambda) - D(\lambda) - \vec{V}\cdot\nabla CKE(\lambda). \tag{4}$$

The cumulus kinetic energy, CKE, is the vertically-integrated kinetic energy in the sub-ensemble interval $[\lambda, \lambda + d\lambda]$ per unit area. The horizontal area over which CKE is integrated is the same as the cloud-base mass flux. CKE includes both the horizontal and vertical components of kinetic energy. The rate at which CKE is dissipated per unit cloud-base mass flux is given by D. Shear production terms have been neglected. Since CKE is a vertically-integrated quantity, vertical transport terms such as those involving vertical velocity, or advection of CKE by the cloud, do not appear. However, horizontal advection by the mean wind ($\vec{V}$) over the depth of the sub-ensemble λ remains.

Closure involves relating CKE to the cloud-base mass flux according to

$$CKE = \alpha M_B^2, \tag{5}$$

as first proposed by *Arakawa and Xu* (1990) and *Xu* (1991). Also, the dissipation is modelled in a simple way:

$$D = \frac{CKE}{\tau_D}, \tag{6}$$

where τ_D is a dissipation time scale.

A linear prognostic equation for the cloud-base mass flux can be developed from Eq. (4),

$$\frac{\partial M_B}{\partial t} = \frac{A}{2\alpha} - \frac{M_B}{2\tau_D} - \vec{V}M_B. \tag{7}$$

A similar equation could also be derived for the CKE (see Eq. 17).

Given α and τ_D, the sub-ensemble cloud-base mass flux can now be determined. However, the mass flux is averaged over a large scale area. The large-scale area might be more properly defined as the area which encompasses the subsident inflow and outflow circulations of the convection in the ensemble. If we let this area be $\mathcal{A}$, then the area covered by convective cores is $a = \sigma_*\mathcal{A}$. The fraction of the sub-ensemble (σ) we expect in a grid box smaller than $\mathcal{A}$ of size Δ_{xy} is

$$\sigma = \frac{\sigma_*\mathcal{A}}{\Delta_{xy}^2}. \tag{8}$$

The large scale area is parameterized to be a function of the local Rossby radius of deformation including local rotational effects.

We require that the total grid fractional area be invariant to the number of sub-ensembles (number of cloud types with different entrainment values) chosen to represent the ensemble. This is done simply by normalizing the fractional area of each sub-ensemble by the total number of sub-ensembles with cloud tops (detrainment levels) at the same model level. Consequently, if we decrease $\Delta\lambda$, although we will have more clouds detraining in any given model level, the total fractional area will remain independent of the discretization of the ensemble.

We also require that the total cloud fractional area in a grid remain less than or equal to unity. If the total cloud area exceeds the grid area we may interpret this to mean that the grid is completely covered by the ensemble, and that only a fraction of the ensemble mass flux is contained within the grid box.

The cloud-base mass flux in a model grid must be adjusted so as to be consistent with the grid fractional area. In summary, the grid fractional area σ is given by

$$\sigma(\lambda) = \frac{f}{N(\lambda)} \frac{\sigma_* \mathcal{A}}{\Delta_{xy}^2} \tag{9}$$

where σ_* is computed directly from the cloud base mass flux equation, $\mathcal{A}$ is either a fixed area or computed as a function of R_i and $N(\lambda)$ is the number of sub-ensembles which detrain in the same model level as sub-ensemble λ. The variable f is unity as long as the total ensemble cloud area remains below the grid area Δ_{xy}^2. If the cloud area is greater than the grid area, f is a normalization factor such that $\sum \sigma(\lambda) = 1$.

By definition then, the cloud-base mass flux in the grid box (not in the large-scale environment) is

$$M_B^G(\lambda) = \sigma(\lambda)\rho(z_o)w(z_o). \tag{10}$$

We obtain w using a simple one-dimensional plume model similar to *Simpson and Wiggert* (1969) and cloud updraft and downdraft properties from a cumulus ensemble model similar to *AS74*. The environmental properties are obtained by inversion of (1).

The expression for $\sigma(\lambda)$ is the probability density function (PDF) we use to obtain the active population from the ensemble. Note that if the total fractional area of the ensemble is less than unity, and if there is only one λ type cloud detraining at each level, the active population is the ensemble. In all other cases, each λ type cloud is allowed to exist, but only a fraction of its mass flux will be represented. The fraction is dependent on the total area of the ensemble and the number of similar λ clouds which detrain at identical model levels.

One of the major disadvantages of using the prognostic CKE equation is that it becomes a function of the unknown parameter α. Perhaps it is not so surprising since the CKE equation is in essence a turbulent kinetic energy (TKE) equation. Scaling arguments by Randall and Pan suggest that α should range between 10^7 and 10^9. In practice, we have found that α should be much more narrowly defined at around 10^8. Values greater than this result in convection which is incapable of removing any significant part of the CAPE generated by external forcing while values significantly less generate explosive convection which consumes not only CAPE generated by external forcing, but any background CAPE as well.

Extension of this scheme to the mesoscale requires the introduction of an adjustment term which is a function of the areal growth rate of convective ensembles. The adjustment term has the effect of nudging the grid value toward or away from the cloud properties depending on whether the sub-ensemble is expanding or contracting. This is important because as the grid area is decreased towards the mesoscale, the presence of the cloud sub-ensembles introduces larger and larger contributions to the total grid-area averages (e.g., clouds contribute to moistening rather than just drying by subsidence).

Closure of the adjustment terms requires the cloud and environment properties and the time rate of change of sub-ensemble grid fractional area. We obtain the tendency of the fractional area indirectly by taking the time derivative of the cloud base mass flux in the grid box, and assuming a steady state updraft. Then

$$\frac{\partial \sigma(z)}{\partial t} = \frac{\eta(z)}{\rho(z) w(z)} \frac{\partial M_B}{\partial t}. \tag{11}$$

where $\eta(z)$ is the normalized mass flux. Given the tendency of the cloud fractional area and the environment and cloud property, the adjustment term is closed.

3. THE MCS PARAMETERIZATION SCHEME

3.1 The basic approach to MCS parameterization

The MCS parameterization scheme is designed to be interfaced with either deep convection parameterization schemes that are in use in a GCM or the generalized cumulus parameterization scheme described above. Initial testing of the scheme has been done by interfacing it with Randall-Pan's variation on the Arakawa-Schubert scheme.

The cumulus parameterization scheme provides heating, condensed water, ice, and water vapor upon which the mesoscale parameterization feeds. The MCS scheme provides, in turn, heating, moistening,

and momentum transports associated with the more slantwise, ascending and descending flow branches of the MCS. These flow branches can be thought of as a generalization of the well known "front-to-rear" ascending and "rear-to-front" descending flow branches of squall lines. However, many MCSs do not exhibit this simple two-dimensional structure but instead are composed of numerous ascending and descending mesoscale flow branches initiating and emanating in various flanks of the MCS.

To provide data for developing the MCS parameterization scheme, we have performed three-dimensional cloud-resolving simulations of two mesoscale convective systems—one from the tropics (EMEX9) and one from the midlatitudes (PRE-STORM 23-24 June 1985). Multiple nesting of two-way interactive grids permits sufficiently small horizontal grid spacing on the finest grids (1500 m for EMEX9, 2083 m for PRE-STORM) that no convective parameterization scheme is required. In each case, the finest grid covers an area on the order of tens of thousands square kilometers ($\sim$ 18,000 km^2 for EMEX9, $\sim$ 17,000 km^2 for PRE-STORM). We run each simulation for several hours using all grids (4.5 hours for EMEX9, 3.5 hours for PRE-STORM 23-24 June). In both cases, the model simulates organized convection and an adjacent stratiform region. The stratiform region accounts for about 44% of the simulated EMEX9 precipitation and for about 32 % of the simulated PRE-STORM 23-24 June precipitation. Overall, we perform these two simulations in the spirit of the Global Energy and Water Cycle Experiment Cloud Systems Study (GCSS), in which cloud-resolving models are used to assist in the formulation and testing of cloud parameterization schemes for larger-scale models.

Construction of the MCS parameterization scheme requires vertical profiles of various quantities (e.g., phase transformation rates) in conditionally-sampled mesoscale updrafts and downdrafts. The first step in this conditional sampling process is to separate the simulated MCSs into convective and stratiform regions—mesoscale updrafts and downdrafts are confined to the stratiform regions.

We employ the *Tao et al.* (1993) separation technique, in which model grid columns exhibiting a surface precipitation rate twice as large as the average value taken over the surrounding grid columns are identified as convective cells. For each core grid column, all adjacent grid columns are also taken to be convective. In addition, any grid column with a rain rate in excess of 25 mm h^{-1} is considered as convective regardless of the above criteria, and any grid column with no surface precipitation is considered convective if the maximum updraft exceeds 5 ms^{-1}. All other precipitating grid columns are considered to be stratiform. Other separation techniques such as proposed by *Xu* (1995) were also tried with little quantitative differences in the diagnosed fields.

The heating and moistening rates by the mesoscale flow branches are described by the following equations:

$$\frac{d\overline{\theta}}{dt} = \frac{\pi\overline{Q_r}^e}{c_p} + \frac{\pi\sum_{i=1}^{6} L_i\overline{\gamma_i^e}}{c_p} + \frac{\pi\overline{Q_r}^*}{c_p} + \frac{\pi\sum_{i=1}^{6} L_i\overline{\gamma_i^*}}{c_p} - \frac{\partial\overline{\omega'\theta'}}{\partial p} - \nabla\cdot\overline{\mathbf{v}'\theta'} \tag{12}$$

and

$$\frac{d\overline{q}}{dt} = -\sum_{i=1}^{4}\frac{\mid L_i\mid}{L_i}\overline{\gamma_i^e} - \sum_{i=1}^{4}\frac{\mid L_i\mid}{L_i}\overline{\gamma_i^*} - \frac{\partial\overline{\omega'q'}}{\partial p} - \nabla\cdot\overline{\mathbf{v}'\mathrm{q}'}, \tag{13}$$

where Q_r is the radiative heating, c_p is the specific heat at constant pressure, and $\pi = (\frac{p_0}{p})^{\frac{R_d}{c_p}}$, where p_0=100 kPa, and R_d is the gas constant for dry air. The summations represent phase transformations. The values of latent heat include condensation(L_1), evaporation (L_2), deposition (L_3), sublimation (L_4), freezing (L_5), and melting (L_6), respectively. Likewise, the phase transformations include γ_1 (condensation), γ_2 (evaporation), γ_3 (deposition), γ_4 (sublimation), γ_5 (freezing), and γ_6 (melting). Cloud properties and those of their environment are denoted by asterisks and superscripts e, respectively, while primes denote departures from the large-scale average. The thermodynamic part of the mesoscale parameterization problem comes down to formulating the terms on the right-hand sides of the above equations.

To compute fluxes, one needs to recognize that the vertical eddy transport of a property χ is given by

$$\overline{\omega'\chi'} = \sum_{i=1}^{N}(\overline{\omega'\chi'})_i, \tag{14}$$

where

$$(\overline{\omega'\chi'})_i = \frac{a_i\omega_i^{*'}\chi_i^{*'}}{1-a_i} \tag{15}$$

and a_i is the fractional area occupied by clouds of the ith of N sub-ensembles. This is valid only when the cloud fractional area is much less than one.

Large-scale phase transformations due to cumulus drafts or mesoscale flow branches are given by

$$\overline{\gamma_i}^* = \sum_{j=1}^{N} a_j \gamma_{i,j}^*, \tag{16}$$

where $\gamma_{i,j}^*$ is the rate of the ith phase transformation per unit mass in an updraft or downdraft belonging to sub-ensemble j.

Parameterizing the thermodynamic forcing of large-scale flow resulting from mesoscale effects requires making approximations of the vertical distributions of the following mesoscale processes in parameterized mesoscale updrafts and downdrafts: (1) deposition and condensation in mesoscale updrafts, (2) freezing in mesoscale updrafts, (3) sublimation in mesoscale updrafts, (4) sublimation and evaporation in mesoscale downdrafts, (5) melting in mesoscale downdrafts, and (6) mesoscale eddy fluxes of entropy and water vapor. The shapes of the vertical profiles of processes (1)-(6) were obtained from the conditionally- sampled mesoscale updrafts and mesoscale downdrafts within our explicit MCS simulations. Figure 1 illustrates schematically the basic processes parameterized in the model.

3.2 Activation of the MCS parameterization

The decision to activate the MCS parameterization is based on the evolution of the total eddy kinetic energy. The total eddy kinetic energy can be partitioned into contributions from the deep convection (CKE) and the mesoscale circulation branches (MKE). Prognostic equations are then developed for CKE and MKE.

Generalization of the CKE equation (4) to an MCS composed of upright cumuli and stratiform-anvil flow branches is given by

$$\frac{dCKE(\lambda)}{dt} = M_B(\lambda)A(\lambda) - \frac{CKE(\lambda)}{\tau_{DIS}} - S_{ac}(\lambda), \tag{17}$$

where A is the cloud work function defined in Arakawa and Schubert, M_B is cloud base mass flux, τ_{DIS} is the CKE dissipation time, and S_{ac} denotes the auto-conversion of CKE to MKE. Here, we have ignored the horizontal advection term in (4). The MKE equation is given by

$$\frac{dMKE}{dt} = S_{ac} + G_B - G_L + G_S - G_P - \frac{MKE}{\tau_{MKE}}, \tag{18}$$

where

$$G_B = \int_0^\infty g\rho_0[w'(\frac{\theta'}{\overline{\theta}} + 0.608 * q_v)]dZ \tag{19}$$

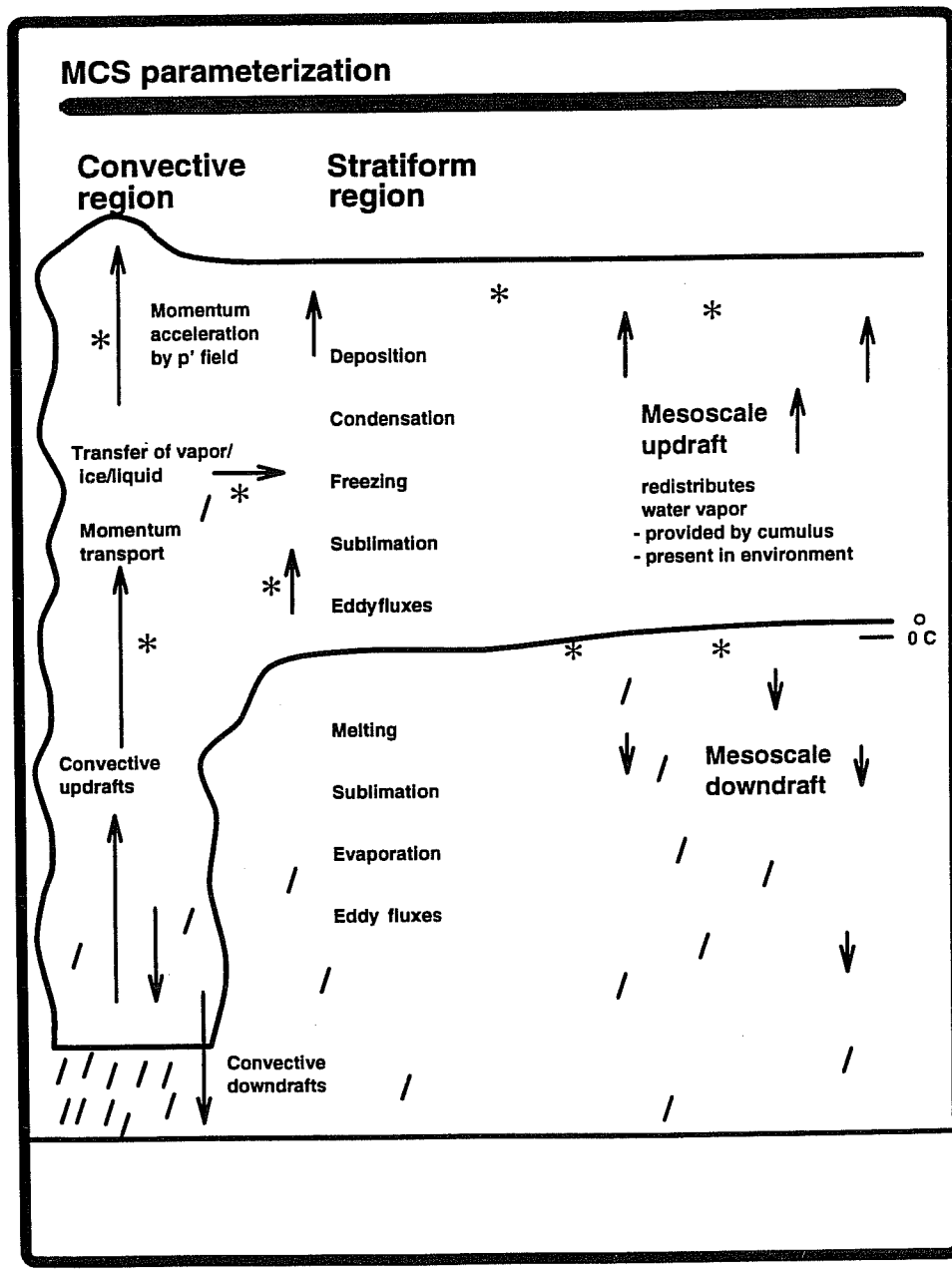

Figure 1: Schematic illustration of the basic processes parameterized in the model.

is thermal buoyancy production rate,

$$G_L = \int_0^\infty g\rho_0[w'q_{total}]dZ \tag{20}$$

is loading buoyancy production rate,

$$G_S = \int_0^\infty \rho_0[\frac{\partial \bar{U}}{\partial Z}\overline{u'w'} + \frac{\partial \bar{V}}{\partial Z}\overline{v'w'})dZ \tag{21}$$

is shear production rate,

$$G_P = \int_0^\infty \rho_0\theta_0[\overline{\frac{\partial \pi'}{\partial X}u'} + \overline{\frac{\partial \pi'}{\partial Y}v'} + \overline{\frac{\partial \pi'}{\partial X}w'}]dZ \tag{22}$$

is pressure gradient force, and τ_{MKE} is the dissipation time of MKE .

We see that CKE is generated primarily by convective updrafts and downdrafts, and once generated, CKE dissipates at a specified rate [O(1h)]. The MKE has two fundamental sources. Some of the CKE generated by the tallest of the deep convection clouds is converted to MKE as the first source, expressed as S_{ac} in (17) which represents the transformation of energy from the initial upright convection to the more slantwise, balanced mesoscale flow branches. If sufficient convection is maintained to generate a certain threshold in MKE, then the MCS scheme is activated. Once activated, the second source accounts for further MKE generation due to mesoscale heating, pressure gradient forces, and shear production within the mesoscale circulation branches of MCSs. The sink of MKE is defined as a simple dissipation term with a dissipation that is slower than ordinary deep convection [O(5h)].

3.3 Parameterization of momentum acceleration

Our conditional sampling of the mesoscale updrafts and downdrafts of the two MCS simulations indicates that the thermodynamic forcing associated with the mesoscale circulations is significant and therefore the effects of such circulations can be profitably included in a convective parameterization scheme. A parallel question which arises is how important are the accelerations of the large-scale horizontal momentum fields by the mesoscale circulations? While there is little question that *convective* drafts can significantly influence the large-scale momentum field (e.g., *Wu and Yanai* 1994), the effect of momentum transport by mesoscale drafts is more questionable.

Previous work suggests that mesoscale drafts are a relatively small component of the momentum budget of MCSs. For example, *Tripoli and Cotton* (1989), who examined the processes responsible for the acceleration of air motion in a numerically simulated MCS, showed that the acceleration of horizontal momentum on the meso-β scale was dominated locally by pressure acceleration that reached peak magnitudes larger than either vertical momentum transport or Coriolis processes by nearly a factor of 4 (see their Fig. 13). Acceleration of horizontal momentum by vertical transport was significant only in their convective core region. As discussed below, analysis of the MCS simulations presented here also indicates that compared to convective updrafts, mesoscale updrafts and downdrafts contribute little to the large-scale acceleration of horizontal momentum.

The magnitude of the impact of subgrid-scale momentum accelerations (including convective and mesoscale components) on the large scale fields may be assessed by the diagnosed momentum budget residual, **F**, which represents the acceleration of the mean flow due to the eddy correlation terms. Following *Wu and Yanai* (1994), the momentum budget equation for the mean flow may be written as

$$\mathbf{F} \equiv \frac{\partial \overline{\mathbf{v}}}{\partial \mathbf{t}} + \overline{\mathbf{v}} \cdot \nabla \overline{\mathbf{v}} + \overline{\omega} \frac{\partial \overline{\mathbf{v}}}{\partial \mathbf{p}} + \nabla \overline{\phi} + \mathbf{fk} \times \overline{\mathbf{v}} = -\nabla \cdot \overline{\mathbf{v}'\mathbf{v}'} - \frac{\partial}{\partial \mathbf{p}} \overline{\mathbf{v}'\omega'}, \tag{23}$$

where $\mathbf{v}$ is the horizontal velocity, ω is the vertical p velocity, ϕ the geopotential, and f the Coriolis parameter. An overbar denotes resolvable (or mean) components and a prime expresses unresolvable (or eddy) components. The two terms on the right-hand side of (23) may be computed for the MCS simulations to obtain a value for the momentum budget residual **F**.

For each simulation, the momentum budget residual resulting from convective drafts far exceeds that resulting from mesoscale drafts. For example, for Grid #3 of the EMEX9 simulation at 1700 UTC, the maximum magnitude of the zonal momentum budget residual for mesoscale drafts at any level is $\sim 0.20 \times 10^{-3}$ ms^{-2} compared to a maximum magnitude of $\sim 0.80 \times 10^{-3}$ ms^{-2} for convective drafts . The values of the meridional momentum budget residual are smaller for both convective and mesoscale drafts, and again the convective drafts have a significantly larger relative contribution than do the mesoscale drafts (see Figure 1). A similar result holds for the PRE-STORM simulation (see Figure 3). There the contribution of mesoscale drafts to the diagnosed momentum budget residual is nearly negligible .

Note, however, that for each simulation, there is still a significant portion of the momentum budget residuals that are unexplained by either conditionally-sampled convective drafts or the mesoscale

(a)

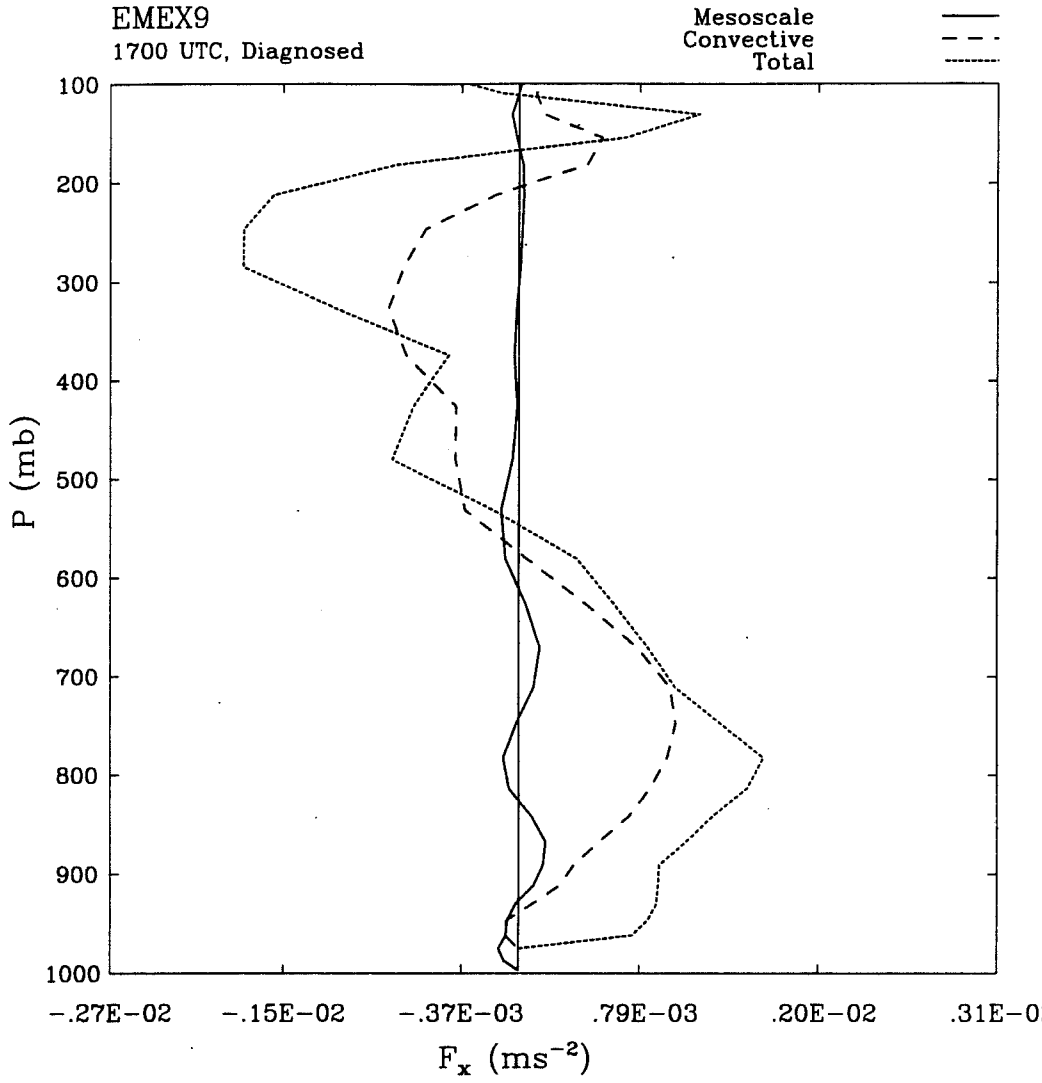

Figure 2: Vertical profiles of the diagnosed (a) zonal and (b) meridional momentum budget residual on Grid #3 of the EMEX9 simulation at 1700 UTC for conditionally sampled convective drafts, mesoscale drafts, and for all grid points.

flow branches. This unexplained acceleration is especially large in the upper troposphere and lower troposphere, and smaller in-between. Scrutiny of the precise grid points included in these regions of unexplained momentum acceleration indicates that in the upper troposphere, wave-like circulations (which can be distant from their convective triggers) are primarily responsible for the unexplained acceleration. However, the relatively large unaccounted-for momentum budget residual in the lower troposphere appears to be an artifact of the convective-region conditional sampling criteria. Because the convective region is defined on a column-by-column basis according to surface precipitation rate, convective updrafts can occasionally be tilted in such a way that they are located just outside the

(b)

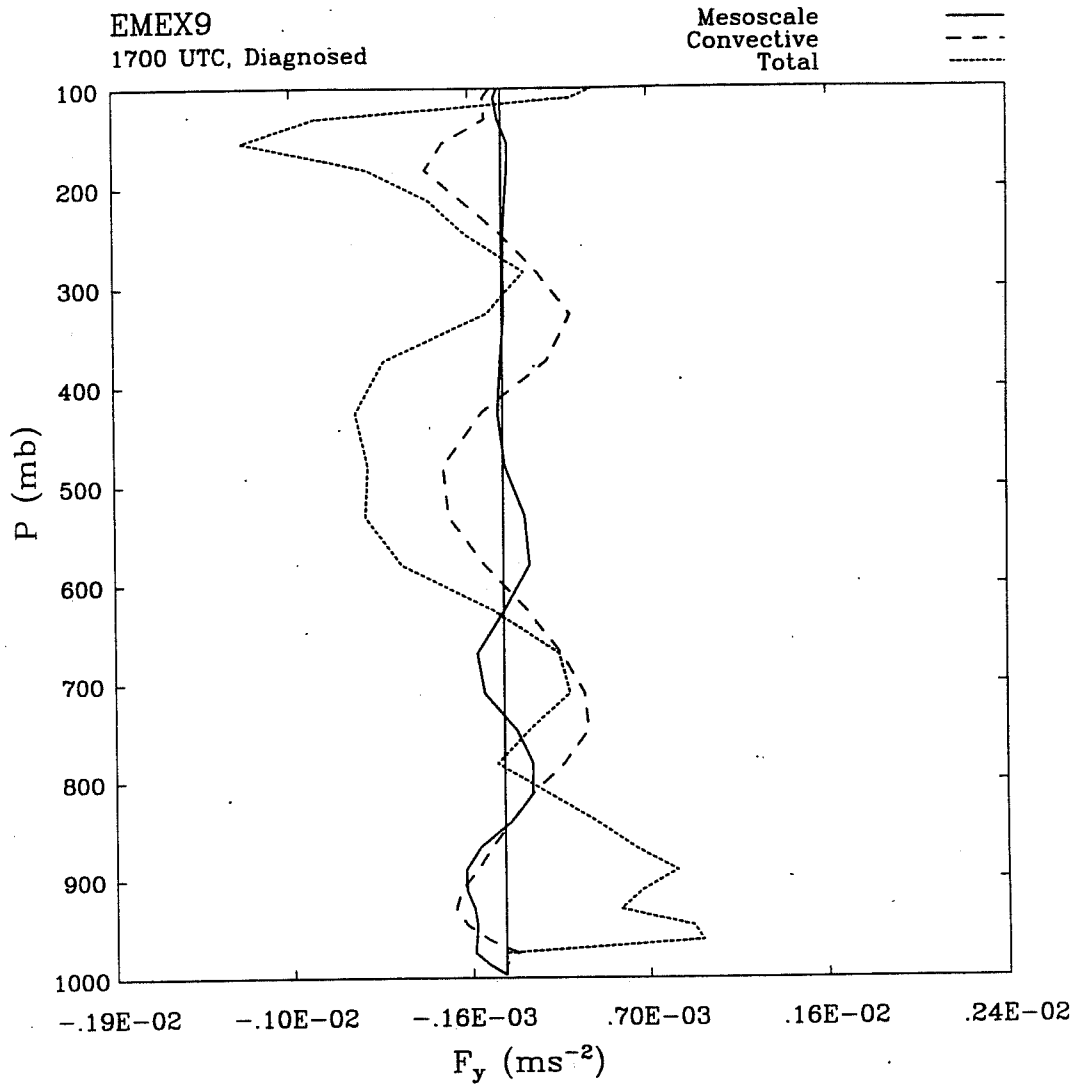

Figure 2: Continued.

conditionally-sampled convective region (the same could theoretically apply to convective downdrafts, too, but our results show that updrafts are the main culprit).

Thus, it appears that in the upper-troposphere, circulations not encompassed by the conditionally-sampled convective region or mesoscale flow branches, such as gravity waves, are responsible for significant large-scale momentum accelerations. Previous studies have shown the importance of convectively-triggered gravity waves to the redistribution of heat and moisture (e.g., *Bretherton and Smolarkiewicz*, 1989); it appears the same may be true for momentum (see, for example, *Fovell et al.*, 1992). Thus, while our results show that it may not be necessary to account for momentum transport by mesoscale drafts *per se* , gravity waves associated with the entire organized MCS could in fact produce significant large-scale momentum accelerations.

(a)

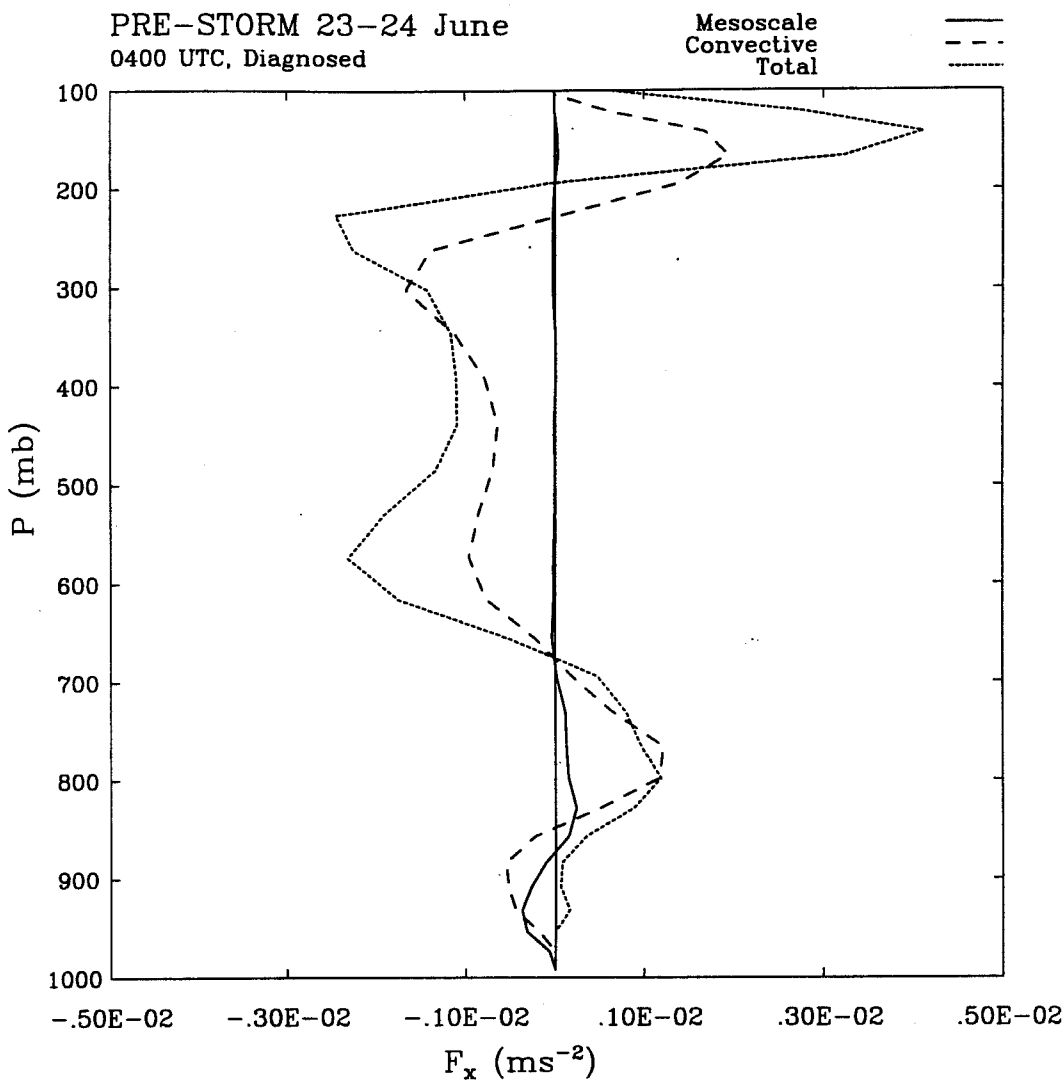

Figure 3: Vertical profiles of the diagnosed (a) zonal and (b) meridional momentum budget residual on Grid #3 of the PRE-STORM simulation at 0400 UTC for conditionally sampled convective drafts, mesoscale drafts, and for all grid points.

Further details about the MCS parameterization scheme can be found in *Alexander* (1995) and *Alexander and Cotton* (1996).

4. TESTING AND EVALUATIONS

Initial testing of the cumulus parameterization scheme has been done by *Rafkin* (1990) for a large number of two- and three-dimensional idealized sea-breeze simulations and compared to corresponding cloud-resolving simulations. Overall the parameterized fields compared quite well with the fields in the CRMs.

(b)

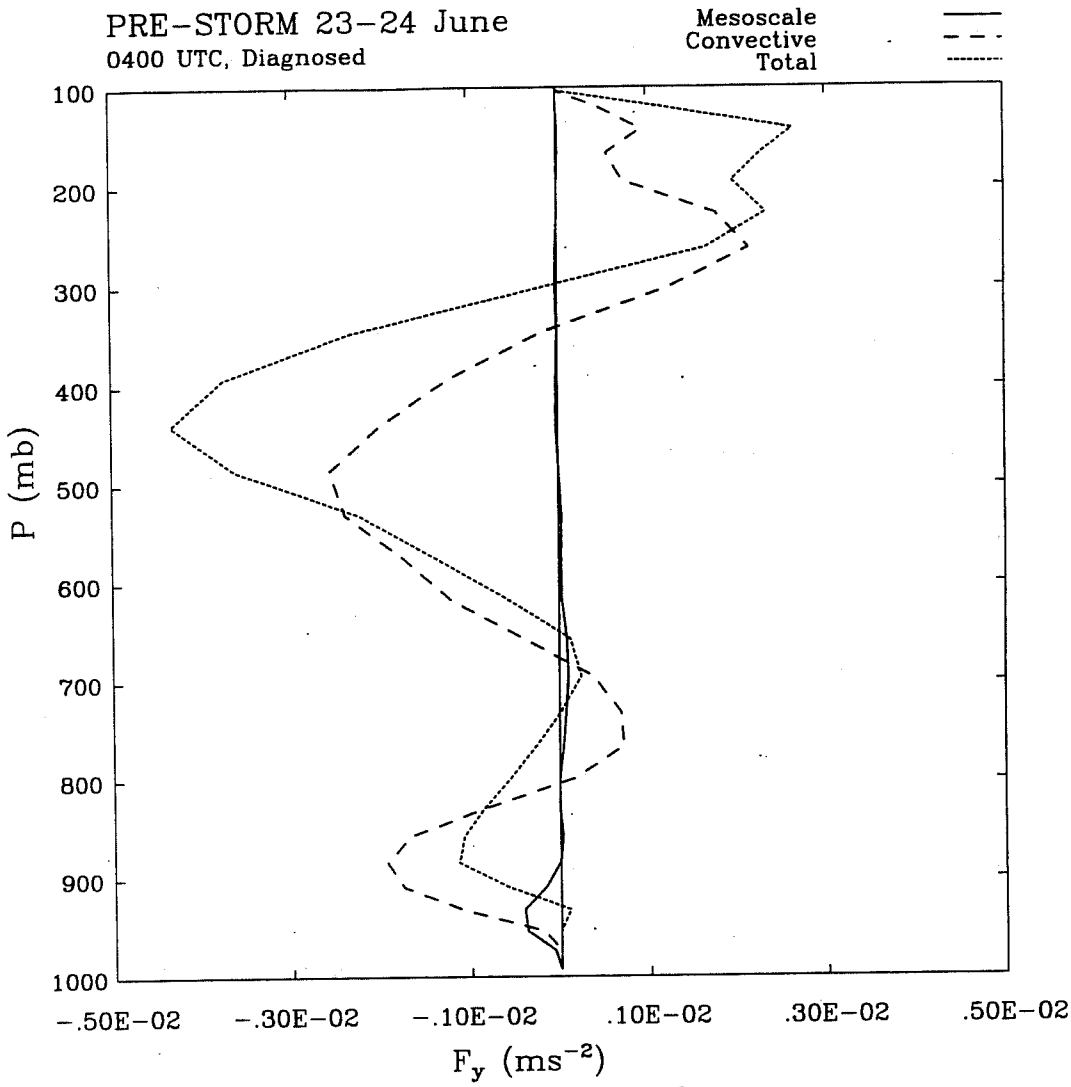

Figure 3: Continued.

Alexander (1995) and *Alexander and Cotton* (1996) used only one hour of cloud-resolved data to obtain the conditionally-sampled variables used in the construction of the MCS scheme. The parameterization was tested, however, on four hours of data for the EMEX9 simulation and three hours of data for the PRE-STORM simulation. Agreement between parameterized and diagnosed heating and drying tendencies is very good for both cases. As an additional test of the sensitivity of the scheme to specified values of the quantities listed above, we use the EMEX9 values of these parameters for a parameterization of PRE-STORM tendencies. As expected, the parameterization does not do quite as good a job of reproducing the exact shapes of the tendency profiles, but the agreement is at least reasonable. In practice, it would be difficult to decide on appropriate values of these "tunable" parameters. The values presented here, along with those presented elsewhere in the published literature, suggest a reasonable range for each parameter, however.

Further evaluations of the coupled cumulus and MCS scheme using independent data sets acquired at the Department of Energy Atmospheric Radiation Measurement Program (DOE-ARM) CART sites were planned. In spite of high technical reviewer comments, it was decided that this project was not relevant to the goals of ARM and not funded for the final testing, evaluation, and refinement stages of the research.

5. ACKNOWLEDGMENTS

This research was supported by the Environmental Sciences Division of U.S.Department of Energy under grant DE-FG03-94ER61749 as part of the Atmospheric Radiation Measurement Program which is part of the DOE Biological and Environmental Research (BER) Program.

6. REFERENCES

Alexander, G David, 1995: The use of simulations of mesoscale convective systems to build a convective parameterization scheme. Atmos Sci Paper #592, Colorado State University, Dept of Atmospheric Science, Fort Collins, CO 232 pp.

Alexander, G David, and William R Cotton, 1996a: The use of cloud-resolving simulations of mesoscale convective systems to build a convective parameterization scheme. J Atmos Sci, Submitted.

Arakawa, A and W H Schubert, 1974: Interaction of a cumulus cloud ensemble with the large-scale environment. Part I. J Atmos Sci, 31, 674-701.

Arakawa, A and K-M Xu, 1990: The macroscopic behavior of simulated cumulus convection and semiprognostic test of the Arakawa-Schubert cumulus parameterization. In: Proc of the Indo-U S seminar on parameterization of sub-grid scale processes in dynamical models of medium-range prediction and global climate. Pune, India.

Bretherton, C S, and P K Smolarkiewicz, 1989: Gravity waves, compensating subsidence and detrainment around cumulus clouds. J Atmos Sci, 46, 740-759.

Fovell, R, D Durran, and J R Holton, 1992: Numerical simulation of convectively generated stratospheric gravity waves. J Atmos Sci, 49, 1427-1442.

Lord, J S, and A Arakawa, 1980: Interaction of a cumulus cloud ensemble with the large-scale environment. Part II. J Atmos Sci, 37, 2677-2692.

Pielke, R A, W R Cotton, R L Walko, C J Tremback, W A Lyons, L D Grasso, M E Nicholls, M D Moran, D A Wesley, T J Lee, and J H Copeland, 1992: A comprehensive meteorological modeling system – RAMS. Meteorol Atmos Phys, 49, 69-91.

Rafkin, Scot C R, 1996: Development of a cumulus parameterization suitable for use in mesoscale through GCM-Scale models. Ph D dissertation, Atmospheric Science Paper #611, Colorado State University, Dept of Atmospheric Science, Fort Collins, CO 80523, 126 pp.

Randall, D A, and D-M. Pan., 1993: Implementation of the Arakawa-Schubert cumulus parameterization with a prognostic closure. Meteorological Monograhps: The representation of cumulus convection in numerical models. ed K.A. Emanuel and D.J. Raymond, 137-144.

Simpson, J and V Wiggert, 1969: Models of precipitating cumulus tower. Mon Wea Rev, 97, 471-489.

Tao, W-K, J Simpson, C-H Sui, B Ferrier, S Lang, J Scala, M-D Chou and K Pickering, 1993: Heating, moisture, and water budgets of tropical and midlatitude squall lines: Comparisons and sensitivity to longwave radiation. J Atmos Sci, 50, 673-690.

Tripoli, G, and W R Cotton, 1989: A numerical study of an observed orogenic mesoscale convective system. Part 1. Simulated genesis and comparison with observations. Mon Wea Rev, 117, 273-304.

Weissbluth, M J, and W R Cotton, 1993: The representation of convection in mesoscale models. Part I: Scheme fabrication and calibration. J Atmos Sci, 50, 3852-3872.

Wu, X, and M Yanai, 1994: Effects of vertical wind shear on the cumulus transport of momentum: Observations and parameterization. J Atmos Sci, 51, 1640-1660.

Xu, K-M 1991: The coupling of cumulus convection with large-scale processes. Ph D Dissertation, University of California, Los Angeles, 250 pp.

Xu, K-M, 1995: Partitioning mass, heat, and moisture budgets of explicitly simulated cumulus ensembles into convective and stratiform components. J Atmos Sci, 52, 551-573.